Magnetoelectric coupling in the multiferroic compound $LiCu_2O_2$

Chen Fang,[1,*] Trinanjan Datta,[2,†] and Jiangping Hu[1,‡]
[1]*Department of Physics, Purdue University, West Lafayette, Indiana 47907, USA*
[2]*Department of Chemistry and Physics, Augusta State University, Augusta, Georgia 30904, USA*
(Received 30 April 2008; revised manuscript received 21 November 2008; published 14 January 2009)

We investigate the possible types of coupling between ferroelectricity and magnetism for the zigzag spin chain multiferroic compound $LiCu_2O_2$. We construct a multi-order-parameter phenomenological model for the material based on a group theoretical analysis. We find that a theory involving interchain magnetoelectric coupling belonging to the same unit cell explains the experimental results of Park *et al.* [Phys. Rev. Lett. **98**, 057601 (2007)]. Our proposed model is able to relate the flop of the spin-spiral plane with the direction of the electric polarization. From our calculations we conclude that the zero-field structure observed by Seki *et al.* [Phys. Rev. Lett. **100**, 127201 (2004)] is the correct one. Furthermore, based on our theoretical model we make specific selection rule predictions about electromagnon excitations present in the $LiCu_2O_2$ system. We predict that the electromagnon peaks measured in an ac-conductivity measurement are field dependent.

DOI: 10.1103/PhysRevB.79.014107 PACS number(s): 77.80.−e, 75.80.+q, 75.47.Lx

I. INTRODUCTION

Cross coupling of magnetism and ferroelectricity in material systems is an intriguing phenomenon. Presently there are chemical compounds in which both magnetism and ferroelectricity can exist simultaneously. These systems are called multiferroics.[1–7] The mixed valent zigzag spin chain cuprate compound $LiCu_2O_2$ was shown to be a multiferroic material by Park *et al.*[8] The experimental data on the compound exhibit a $\pi/2$ flop of the spin-spiral plane for a magnetic field applied along the crystallographic *b* axis.

In this paper we introduce a theoretical model involving an interchain magnetoelectric coupling to provide an explanation for the experimental data on $LiCu_2O_2$.[8–11] For $LiCu_2O_2$, there are two chains in each unit cell. Therefore, there are two types of "interchain" interactions. The first one is the interchain coupling between two chains in two different unit cells. The second one is the interchain coupling between two chains in the same unit cell. While the first one is self-evident due to the observation of magnetic order, the second one is not. The second type of interchain coupling plays an important role in $LiCu_2O_2$ based on the analysis given in our paper. We show that a different set of magnetoelectric couplings can be generated by the second type of interchain couplings.

We perform a group theoretical calculation[12–15] for the $LiCu_2O_2$ magnetic structure. Based on that analysis we construct a phenomenological multi-order-parameter magnetization model (see Sec. IV). There have also been other theoretical efforts to explain the experimental data.[16,17] The multi-order-parameter model is able to account for the electric polarization flip through $\pi/2$ and relate the flop of the spin-spiral plane with the direction of the electric polarization (see Sec. V). The theory does not include any anisotropic terms. Besides accounting for the observed experimental features (polarization flip and spin-spiral plane flop), we also discuss the consequences of twinning of the crystal structure for our theory, and derive a selection rule associated with the low energy hybrid excitations of phonon and magnon, termed as electromagnons.

We demonstrate through our calculations that one of the experimental facts, electric polarization along the *a* axis, should be ascribed to interchain interactions generated as a result of considering the details of the magnetic unit cell. We show that not all the magnetoelectric interaction terms have the usual phenomenological form.[18] Specifically, the interchain coupling term cannot be expressed as a $\vec{P}\cdot[(\vec{M}\cdot\vec{\nabla})\vec{M}-(\vec{\nabla}\cdot\vec{M})\vec{M}]$ term in the continuum limit. A hidden assumption behind the continuum coupling model is that the magnetic order is described by a single order parameter. When the lattice structure is complicated this assumption is not valid and the general form of the magnetoelectric coupling can be different.

This paper is arranged as follows. In Sec. II we describe the crystal and the magnetic structure of $LiCu_2O_2$. In Sec. III we elucidate the magnetic symmetry operations of the lattice, and use group theoretical arguments to construct the possible intrachain and interchain couplings. In Sec. IV we derive the phenomenological magnetization model. In Sec. V we analyze the model derived in Sec. IV to provide an explanation for the experimental data of Park *et al.*[8] In Sec. VI we derive the consequences of the various spin structures and electric polarization within our model. In Sec. VII we discuss the experimental consequences of twinning. In Sec. VIII we derive the selection rule for electromagnons. Finally, in Sec. IX we provide a summary and the main conclusions of our paper.

II. $LiCu_2O_2$ SYSTEM

The mixed valent cuprate compound $LiCu_2O_2$ is a ferroelectric material. It crystallizes in an orthorhombic structure with the space group *Pnma* (No. 62).[19–21] The crystal structure of the compound can be visualized as follows. Consider two linear Cu^{2+} chains propagating along the crystallographic *b* axis. The two chains are displaced $b/2$ with respect to each other and they form a zigzag triangular ladderlike structure as shown in Fig. 1. The ladders are separated from each other by the nonmagnetic Li^+ ions and by the layers of nonmagnetic Cu^+ ions. The letters *a*, *b*, and *c* represent the lattice constants of the simple orthorhombic crystal structure.

The magnetic behavior of the system is provided by the Cu^{2+} ions which carry a spin 1/2. The magnetic structure of

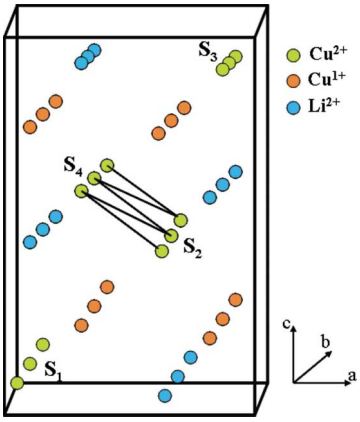

FIG. 1. (Color online) $LiCu_2O_2$ crystal structure: the multiferroic $LiCu_2O_2$ compound has pairs of Cu^{2+}-ion chains running parallel to each other along the b axis. Each chain is separated from the other by $b/2$ and forms the zigzag triangular ladder structure shown in the figure. The bold line indicates the bond between the spin-1/2 magnetic Cu^{2+} ions (represented by the green dots) forming the zigzag chain. These ladders are separated from each other by the nonmagnetic Li^+ ions (represented by the blue dots) and by the layers of nonmagnetic Cu^+ ions (represented by the orange dots). In $LiCu_2O_2$ there are four spatially inequivalent magnetic ions in the magnetic unit cell that we consider in our theoretical formulation (see Secs. III and IV). They are denoted as $\vec{S}_1$, $\vec{S}_2$, $\vec{S}_3$, and $\vec{S}_4$ in the figure above.

$LiCu_2O_2$ has been determined from the neutron-scattering experiments.[9,10] While the neutron-diffraction experiments of Masuda *et al.*[10] concluded that the rotating spins lie in the *ab* plane, Seki *et al.*[9] indicated that the spins lie in the *bc* plane. There is also independent NMR study which observes an out-of-plane component.[11] The magnetic modulation vector obtained from the experiments is $\vec{Q}=(0.5\frac{2\pi}{a},\frac{2\pi\xi}{b},0)$, where $\xi=0.174$ is the spiral modulation along the chain direction. Along the a axis there is an antiferromagnetic order and along the b axis there is a spiral order. Successive spins on each rung are almost parallel to each other with each spin being rotated relative to each other by an angle $\alpha=2\pi\xi$. Within each double chain any nearest-neighbor spin from the opposite legs are almost antiparallel and form an angle $\alpha/2=\pi\xi$.

III. SYMMETRY OPERATIONS OF THE LATTICE AND MAGNETIC STRUCTURE

The goal of this section is to find a physically appropriate form for the magnetoelectric coupling in $LiCu_2O_2$ subject to the symmetry constraints of the magnetic structure. Such a term should conserve translational, space inversion (if it is also an element of the space group, which is the case for $LiCu_2O_2$), and time-reversal symmetries. Phenomenological models[18] for multiferroics are based on these considerations only. These models assume that a single unit cell of the lattice is a point in the system without any structure. An appropriate realistic model in these cases should include all the inequivalent atoms (considering both the type and the location of the ion in space) in a single magnetic unit cell. This allows for the possibility to include more degrees of freedom. For example, in the $LiCu_2O_2$ case there are four spatially inequivalent magnetic ions in the magnetic unit cell that we should consider. They are denoted as $\vec{S}_1$, $\vec{S}_2$, $\vec{S}_3$, and $\vec{S}_4$ (see Fig. 1).

As the number of possible forms of the magnetoelectric coupling increases rapidly with the degrees of freedom, such a detailed model seems too complicated to be useful. However there are symmetry constraints which help in simplifying the situation. These constraints should be obeyed by all the terms in the Hamiltonian. The terms should be invariant under the lattice symmetry operations and time-reversal symmetry. The lowest-order magnetoelectric coupling which preserves time-reversal symmetry is a trilinear term.[12–15] It is linear in the electric polarization and bilinear in the magnetic order parameters. To simplify the discussion, we consider the coupling terms that involve the uniform spontaneous electric polarization $\vec{P}$ and not those that include the modulations of the polarization. The general magnetoelectric Hamiltonian H_{ME} is then

$$H_{\mathrm{ME}}=\sum_{\alpha}\lambda_{\alpha}P_{\alpha}\sum_{ij;\beta\gamma}\sum_{\vec{R}\vec{R}'}C_{ij;\alpha\beta\gamma}(\vec{R}-\vec{R}')S_i^{\beta}(\vec{R})S_j^{\gamma}(\vec{R}'), \quad (1)$$

where λ^{α} is the magnetoelectric coupling, $C_{ij;\alpha\beta\gamma}$ is a general coefficient in the Hamiltonian, $\alpha,\beta,\gamma=a,b,c$ are the indices for the crystallographic axes, $i,j=1,2,3,4$ are the indices for the four spatially inequivalent magnetic ions in the magnetic unit cell (see Fig. 1), and $\vec{R}$ denotes the position in the unit cell. Also, the α spin component for the ith magnetic atom at a position $\vec{R}$ in the magnetic unit cell is represented by $S_j^{\alpha}(\vec{R})$. The Fourier-transformed version of the Hamiltonian is

$$H_{\mathrm{ME}}=\sum_{\alpha}\lambda_{\alpha}P_{\alpha}\sum_{ij;\beta\gamma}[C_{ij;\alpha\beta\gamma}(\vec{Q})S_i^{\beta}(\vec{Q})S_j^{\gamma}(-\vec{Q})+\mathrm{c.c.}], \quad (2)$$

where $C_{ij;\alpha\beta\gamma}(\vec{Q})$ is the Fourier transform of $C_{ij;\alpha\beta\gamma}(\vec{R}-\vec{R}')$ and $S_i^{\alpha}(\vec{Q})$ is the Fourier transform of the spin components. The above equation was obtained by substituting the Fourier-transformed version of the magnetic structure $S_i^{\alpha}(\vec{R})=S_i^{\alpha}(\vec{Q})\exp(i\vec{Q}\cdot\vec{R})+\mathrm{c.c.}$ into Eq. (1).

Not every term in the above magnetoelectric coupling conserves all the symmetries. Only certain linear combinations do. Specifically we are interested in the lattice symmetry operations that conserve the magnetic structure with the magnetic propagation vector $\vec{Q}$. From group representation theory we know that these operations constitute a subgroup of the full symmetry group of the lattice for which we have one (and only one) two-dimensional (2D) representation, E, 2_b, m_c, and m_c2_b all being two-by-two matrices.

The lattice symmetry operations which preserve the magnetic propagation vector $\vec{Q}$ are listed in Table I. The two-dimensional representations of the symmetry operations are given by

TABLE I. Lattice symmetry operations which preserve the magnetic propagation vector $\vec{Q}$. The identity operation is represented by E. A twofold rotation about the crystallographic b axis is represented by 2_b. A reflection about the c axis is denoted by m_c, and finally a combination of the rotation and reflection is denoted by $m_c 2_b$.

$E\vec{r}=(x,y,z)$
$2_b\vec{r}=(\bar{x},y+1/2,\bar{z})$
$m_c\vec{r}=(x-1/2,y,\bar{z}-1/2)$
$m_c 2_b\vec{r}=(\bar{x}-1/2,y+1/2,z-1/2)$

$$E=\begin{pmatrix}1 & 0\\ 0 & 1\end{pmatrix};2_b=\begin{pmatrix}-e^{-iqb/2} & 0\\ 0 & e^{-iqb/2}\end{pmatrix}, \tag{3}$$

$$m_c=\begin{pmatrix}0 & -1\\ 1 & 0\end{pmatrix};m_c 2_b=\begin{pmatrix}0 & -e^{-iqb/2}\\ -e^{-iqb/2} & 0\end{pmatrix}. \tag{4}$$

For the above representation we can find groups of symmetry adapted variables which are transformed according to the representation under the symmetry operations. A symmetry adapted variable is a column vector (two dimensional in this case) whose elements are a linear combination of the original magnetic variables—$S_i^{\alpha}(\vec{Q})$'s. The variables transform under any operation of the subgroup in the same way they transform if left multiplied by the corresponding matrix for the same operation. These variables can be computed for the $LiCu_2O_2$ case after deducing the transformation tables (see Tables II and III) for all the members of the symmetry subgroup. The symmetry operation table for $m_c 2_b$ can be obtained by combining Tables II and III.

TABLE III. Symmetry operation: m_c, reflection about the crystallographic c axis. In $LiCu_2O_2$ there are four spatially inequivalent magnetic ions in the magnetic unit cell. They are denoted as $\vec{S}_1$, $\vec{S}_2$, $\vec{S}_3$, and $\vec{S}_4$ (see Fig. 1). The subscripts a, b, and c denote the components along those crystallographic axes.

S_1	S_2	S_3	S_4
$S'_{1a}=-S_{2a}$	$S'_{2a}=S_{1a}$	$S'_{3a}=S_{4a}$	$S'_{4a}=-S_{3a}$
$S'_{1b}=-S_{2b}$	$S'_{2b}=S_{1b}$	$S'_{3b}=S_{4b}$	$S'_{4b}=-S_{3b}$
$S'_{1c}=S_{2c}$	$S'_{2c}=-S_{1c}$	$S'_{3c}=-S_{4c}$	$S'_{4c}=-S_{3c}$

We find six groups of symmetry adapted variables, that is, twelve elements in total. The number of symmetry adapted vectors can also be deduced if we notice the fact that all the elements should make a different basis for the magnetic structure. This requires a total number of twelve elements, the same as the original number of S_i^{α}'s. The total number of vectors will be six. We sort them into two sets as listed below. The groups of symmetry adapted variables, $\mathcal{S}^{(1)}$ and $\mathcal{S}^{(2)}$, are then

$$\mathcal{S}^{(1)}=\left\{\begin{pmatrix}S_{1a}+e^{-iqb/2}S_{3a}\\ S_{2a}-e^{-iqb/2}S_{4a}\end{pmatrix},\begin{pmatrix}S_{1b}-e^{-iqb/2}S_{3b}\\ S_{2b}+e^{-iqb/2}S_{4b}\end{pmatrix},\begin{pmatrix}S_{2c}+e^{-iqb/2}S_{4c}\\ S_{1c}-e^{-iqb/2}S_{3c}\end{pmatrix}\right\}, \tag{5}$$

$$\mathcal{S}^{(2)}=\left\{\begin{pmatrix}S_{2a}+e^{-iqb/2}S_{4a}\\ -S_{1a}+e^{-iqb/2}S_{4a}\end{pmatrix},\begin{pmatrix}S_{2b}-e^{-iqb/2}S_{4b}\\ -S_{1b}-e^{-iqb/2}S_{3b}\end{pmatrix},\begin{pmatrix}S_{1c}+e^{-iqb/2}S_{3c}\\ -S_{2c}+e^{-iqb/2}S_{4c}\end{pmatrix}\right\}. \tag{6}$$

Using the properties of the symmetry adapted variables, we then have

$$\mathcal{S}_{\beta}^{(i)\dagger}M_{ij;\beta\gamma}\mathcal{S}_{\gamma}^{(j)}\xrightarrow{2_b}\mathcal{S}_{\beta}^{(i)\dagger}(m_{2_b})^{\dagger}M_{ij;\beta\gamma}m_{2_b}\mathcal{S}_{\gamma}^{(j)}=\mathcal{S}_{\beta}^{(i)\dagger}(\sigma_z M_{ij;\beta\gamma}\sigma_z)\mathcal{S}_{\gamma}^{(j)}, \tag{7}$$

TABLE II. Symmetry operation: 2_b, twofold rotation about the crystallographic b axis. In $LiCu_2O_2$ there are four spatially inequivalent magnetic ions in the magnetic unit cell. They are denoted as $\vec{S}_1$, $\vec{S}_2$, $\vec{S}_3$, and $\vec{S}_4$ (see Fig. 1). The subscripts a, b, and c denote the components along those crystallographic axes.

S_1	S_2	S_3	S_4
$S'_{1a}=-S_{3a}e^{-iqb/2}$	$S'_{2a}=-S_{4a}e^{-iqb/2}$	$S'_{3a}=-S_{1a}$	$S'_{4a}=-S_{2a}$
$S'_{1b}=-S_{3b}e^{-iqb/2}$	$S'_{2b}=S_{4b}e^{-iqb/2}$	$S'_{3b}=S_{1b}$	$S'_{4b}=S_{2b}$
$S'_{1c}=-S_{3c}e^{-iqb/2}$	$S'_{2c}=-S_{4c}e^{-iqb/2}$	$S'_{3c}=-S_{1c}$	$S'_{4c}=-S_{2c}$

$$\mathcal{S}_{\beta}^{(i)\dagger}M_{ij;\beta\gamma}\mathcal{S}_{\gamma}^{(j)}\xrightarrow{m_c}\mathcal{S}_{\beta}^{(i)\dagger}(m_{m_c})^{\dagger}M_{ij;\beta\gamma}m_{m_c}\mathcal{S}_{\gamma}^{(j)}=\mathcal{S}_{\beta}^{(i)\dagger}(\sigma_y M_{ij;\beta\gamma}\sigma_y)\mathcal{S}_{\gamma}^{(j)}. \tag{8}$$

Hereafter we suppress the argument of $\mathcal{S}$. We will consider $\mathcal{S}$ to be $\mathcal{S}(\vec{Q})$ and $\mathcal{S}^{\dagger}$ to be $\mathcal{S}(-\vec{Q})$. Having found the symmetry adapted variables, we recast the magnetoelectric Hamiltonian in the following form:

$$H_{\mathrm{ME}}=\sum_{\alpha}\lambda_{\alpha}P_{\alpha}\sum_{i,j;\beta,\gamma}\mathcal{S}_{\beta}^{(i)\dagger}M_{ij;\beta\gamma}\mathcal{S}_{\gamma}^{(j)}+\mathrm{c.c.}, \tag{9}$$

where the indices $i,j=1,2$ are for the symmetry adapted variables and $M_{ij;\beta\gamma}$ is an arbitrary two-by-two coupling matrix. We apply the stated constraints to find all the possible forms of the magnetoelectric coupling:

(1) *Time-reversal symmetry.* The expression above with its trilinearity automatically includes time-reversal symmetry.

(2) *Lattice symmetry.* We focus on the subgroup of the lattice symmetry operations. All three components of the electric polarization behave differently under the symmetry operations. We discuss each case separately. In the following we explicitly work out the case for P_c and simply list the result for the other two components. The symmetry properties of P_c under the lattice symmetry operations are $P_c \overset{m_c}{\rightarrow} -P_c$, $P_c \overset{2_b}{\rightarrow} -P_c$, and $P_c \overset{I}{\rightarrow} -P_c$. From the overall invariance of the trilinear coupling, we require that $M_{ij;\beta\gamma}$ anticommute with both σ_y and σ_z. From this we can infer that M_{ij} should be proportional to σ_x to preserve the invariance under symmetry operations. A similar procedure can be applied to find the appropriate M_{ij}'s for P_a and P_b. The result can be summarized as follows: for P_a, $M_{ij} \propto \sigma_y$; for P_b, $M_{ij} \propto 1$; for P_c, $M_{ij} \propto \sigma_x$. Later we will prove that the constant of proportionality can be either real or purely imaginary based on space inversion symmetry arguments.

(3) *Inversion symmetry.* Inversion operation is *not* a member of the subgroup of the symmetry operations that conserves the magnetic propagation vector $\vec{Q}$. Therefore it cannot be represented by a matrix acting on the symmetry adapted variables. The mapping for space inversion operation is

$$S_1^\alpha(q) \rightarrow S_3^\alpha(-q), \quad S_2^\alpha(q) \rightarrow S_4^\alpha(-q), \tag{10}$$

$$S_3^\alpha(q) \rightarrow S_1^\alpha(-q), \quad S_4^\alpha(q) \rightarrow S_2^\alpha(-q), \tag{11}$$

where α denotes the spin component. With this mapping we obtain the expression for the inversion operation in terms of the symmetry adapted variables as

$$I\mathcal{S}_b^{(i)} = \begin{pmatrix} -e^{-iqb/2} & 0 \\ 0 & e^{-iqb/2} \end{pmatrix} \mathcal{S}_b^{(i)*}, \tag{12}$$

$$I\mathcal{S}_\alpha^{(i)} = \begin{pmatrix} e^{-iqb/2} & 0 \\ 0 & -e^{-iqb/2} \end{pmatrix} \mathcal{S}_\alpha^{(i)*}, \tag{13}$$

where $\alpha = a, c$ and $i = 1, 2$ are the indices for the symmetry adapted variables. Below we explicitly work out the case for P_c and list the result for the other two components of electric polarization. We have

$$P_c \mathcal{S}_\beta^{(i)\dagger} \sigma_x \mathcal{S}_\gamma^{(j)} \overset{I}{\rightarrow} (-P_c)(\mathcal{S}_\beta^{(i)T} \sigma_z \sigma_x \sigma_z \mathcal{S}_\gamma^{(j)*}) = P_c (\mathcal{S}_\beta^{(i)\dagger} \sigma_x \mathcal{S}^{(j)})^*, \tag{14}$$

if β, $\gamma = a$, c, or $\beta = \gamma = b$, and

$$P_c \mathcal{S}_\beta^{(i)\dagger} \sigma_x \mathcal{S}_\gamma^{(j)} \overset{I}{\rightarrow} (-P_c)(-\mathcal{S}_\beta^{(i)T} \sigma_z \sigma_x \sigma_z \mathcal{S}_\gamma^{(j)*}) = -P_c (\mathcal{S}_\beta^{(i)\dagger} \sigma_x \mathcal{S}_\gamma^{(j)})^*, \tag{15}$$

if either β or γ is b. The electric polarization and the total Hamiltonian must be real, making the proportionality constant in the first case real and in the second case purely imaginary. The complete result is summarized below. It shows that there are only six forms that do not violate any of the symmetries of the system

$$P_a[\mathcal{S}_\beta^{(i)\dagger} \sigma_y \mathcal{S}_\gamma^{(j)} + \text{c.c.}], \tag{16}$$

$$P_b[\mathcal{S}_\beta^{(i)\dagger} \mathcal{S}_\gamma^{(j)} + \text{c.c.}], \tag{17}$$

$$P_c[\mathcal{S}_\beta^{(i)\dagger} \sigma_x \mathcal{S}_\gamma^{(j)} + \text{c.c.}], \tag{18}$$

if β, $\gamma = a$, c, or $\beta = \gamma = b$, and

$$iP_a[\mathcal{S}_\beta^{(i)\dagger} \sigma_y \mathcal{S}_\gamma^{(j)} - \text{c.c.}], \tag{19}$$

$$iP_b[\mathcal{S}_\beta^{(i)\dagger} \mathcal{S}_\gamma^{(j)} - \text{c.c.}], \tag{20}$$

$$iP_c[\mathcal{S}_\beta^{(i)\dagger} \sigma_x \mathcal{S}_\gamma^{(j)} - \text{c.c.}], \tag{21}$$

if either β or γ is b.

To summarize our work up to this point, we have derived all the possible forms of magnetoelectric coupling that are invariant under (1) time reversal, (2) space inversion, and (3) the lattice symmetry operations that conserve the magnetic propagation vector by using the symmetry adapted variables.

IV. PHENOMENOLOGICAL MAGNETIZATION MODEL

In this section we focus on simplifying the form for the magnetoelectric coupling derived in Sec. III. We classify the simplified magnetoelectric interactions as intrachain and interchain terms. The latter is a signature of the double-chain structure of $LiCu_2O_2$.

A. Model simplification

A simplified expression for the phenomenological model can be obtained if we observe first that ferroelectricity coexists with noncollinear magnetic structure. This suggests that terms with $\beta = \gamma$ can be excluded. Second, the polarization along the b axis is not observed. Therefore, the couplings with P_b need not be considered. Third, the magnetic moments on the four Cu^{2+} atoms, assumed to be independent variables in our theoretical formulation, form two zigzag chains[19–21] extended in the b direction on each of which a spin-density wave with a propagation vector q along the b axis exists. To be specific we have S_2 and S_4 on one zigzag chain, and S_1 and S_3 in the adjacent unit cell on another zigzag chain (see Fig. 1). This observation immediately leads to

$$S_{1\alpha} = e^{-iqb/2} S_{3\alpha}, \tag{22}$$

$$S_{2\alpha} = -e^{-iqb/2} S_{4\alpha}. \tag{23}$$

Moreover the symmetry adapted variables become

$$\mathcal{S}^{(1)} = \left\{ \begin{pmatrix} 2e^{-iqb/2} S_{3a} \\ -2e^{-iqb/2} S_{4a} \end{pmatrix}, \begin{pmatrix} 0 \\ 0 \end{pmatrix}, \begin{pmatrix} 0 \\ 0 \end{pmatrix} \right\}, \tag{24}$$

$$\mathcal{S}^{(2)} = \left\{ \begin{pmatrix} 0 \\ 0 \end{pmatrix}, \begin{pmatrix} -2e^{-iqb/2} S_{4b} \\ -2e^{-iqb/2} S_{3b} \end{pmatrix}, \begin{pmatrix} 2e^{-iqb/2} S_{3c} \\ 2e^{-iqb/2} S_{4c} \end{pmatrix} \right\}. \tag{25}$$

All the magnetoelectric coupling terms can be enumerated in terms of the symmetry adapted variables by using the above two equations, Eqs. (24) and (25). After the insertion of Eqs.

(22) and (23) three of the six symmetry adapted variables reduce to zero. We can then write them into a single two-column three-component variable

$$\mathcal{M} = \left\{ \begin{pmatrix} M_{(1)a} \\ -M_{(2)a} \end{pmatrix}, \begin{pmatrix} -M_{(2)b} \\ -M_{(1)b} \end{pmatrix}, \begin{pmatrix} M_{(1)_c} \\ M_{(2)_c} \end{pmatrix} \right\}. \quad (26)$$

In the above expression we have defined $M_{(1)\alpha}=2e^{-iqb/2}S_{3\alpha}$ to represent the magnetization in the first chain and $M_{(2)\alpha}=2e^{-iqb/2}S_{4\alpha}$ to represent the magnetization in the second chain. All the spin variables are the Fourier components of the real-space magnetic structure and are in general complex numbers. After these simplifications, the general magnetoelectric terms [Eqs. (16)–(21)] are reduced to intrachain interaction terms

$$P_a[M^*_{(1)a}M_{(1)b} + M^*_{(1)b}M_{(1)a} + (1) \to (2)], \quad (27)$$

$$P_a[M^*_{(1)c}M_{(1)b} + M^*_{(1)b}M_{(1)c} - (1) \to (2)], \quad (28)$$

$$iP_c[M^*_{(1)a}M_{(1)b} - M^*_{(1)b}M_{(1)a} - (1) \to (2)], \quad (29)$$

$$iP_c[M^*_{(1)c}M_{(1)b} - M^*_{(1)b}M_{(1)c} + (1) \to (2)], \quad (30)$$

and interchain interaction terms

$$iP_a[M^*_{(1)a}M_{(2)c} + M^*_{(2)a}M_{(1)c} - M_{(1)a}M^*_{(2)c} - M_{(2)a}M^*_{(1)c}], \quad (31)$$

$$P_c[M^*_{(1)a}M_{(2)c} - M^*_{(2)a}M_{(1)c} + M_{(1)a}M^*_{(2)c} - M_{(2)a}M^*_{(1)c}]. \quad (32)$$

We will discuss the six terms above [Eqs. (27)–(32)] in Sec. IV B. We realize from their expressions that the first four are intrachain terms since every term has two magnetization components from the same chain. The last two are interchain ones.

B. Intrachain versus interchain couplings

First we focus on the intrachain couplings. A theory that has these terms assumes that, aside from the possible spin exchange between spin chains, each chain is contributing to the ferroelectricity identically and independently. Examples of these include theories which have explained multiferroic systems such as the 113 perovskites,[22] $Ni_3V_2O_8$,[7] and $RbFe(MnO_4)_2$.[23] In $LiCu_2O_2$, we would like to see what predictions these intrachain terms can make and compare them to experiments.

We adopt the magnetic structure proposed by Park *et al.*[8] and Seki *et al.*,[9] where there is a spin spiral whose components lie on the *bc* plane, propagating in the *b* axis, at zero magnetic field. Furthermore, we notice that we do not know the relative phase between the two spin chains. To make progress we therefore make an assumption. Let us consider the two spin chains to be either *in phase* or *out of phase*. This implies that $M_{(1)\alpha}=\pm M_{(2)\alpha}$. This is true if we adopt the spin model proposed in Ref. 24, where the spin chains are in phase if the interaction between the double chains $J_\perp<0$ and out of phase if $J_\perp>0$. Using this magnetic structure one easily obtains $M_{(i)a}=0$, $M_{(i)b}=1$, and $M_{(i)c}=i$. Substituting these back to the intrachain coupling terms, we find that only the P_c term [Eq. (30)] can be nonzero. This is in accordance with the experiments.[8]

We now focus on the interchain terms. These terms have zero contributions at zero field, as all these terms involve the *a* component of spins, which is zero at zero field. However, the spins may flop to other planes upon applying a magnetic field along the *b* axis. If we assume that the spins are flopped to the *ac* plane, then these interchain terms immediately produce a nonzero P_a from Eq. (31). We therefore conclude that the interchain term does explain the ferroelectricity generated in nonzero magnetic field. The presence of interchain coupling is supported by experimental evidence found in Raman-scattering experiment.[25]

We have compared the known experimental data and the predictions obtained by both the intrachain and the interchain magnetoelectric couplings. We see that the theory must include at least two terms: Eq. (30) from intrachain couplings and Eq. (31) from the interchain couplings, to account for the zero-field and nonzero-field data, respectively. The other terms may exist but do not contribute to the static ferroelectricity, and their presence will *not* be considered in Sec. V where we consider a minimal-coupling model.

It is useful for further calculation and understanding to write down the magnetoelectric couplings in the continuum real space rather than the *k* space. All the symmetry allowed magnetoelectric couplings are given in terms of the Fourier components of the spins. In transforming them into real space to obtain a continuum theory for further study, it can be shown that the real-space expression is not unique. The reason is that in writing down any magnetoelectric coupling term, taking the term $iP_c[M^*_{(1)b}M_{(1)c,a}-\text{c.c.}\pm(1)\to(2)]$ as an example, the coefficient before this term can be an arbitrary function of the modulation vector q. [It should be pointed out that the value of the wave vector q here is not the experimental $(2\pi)0.826$ but its physically equivalent value $q=(0.826-1)2\pi=-0.174(2\pi)$, which is consistent with the continuum limit we are considering.] The symmetry alone cannot give us any property of such a function besides that $f(q)$ is odd under $q\to-q$ if there is a prefactor i in front of the magnetoelectric coupling, and even if there is no i. For the example considered above, we have $f(q)=f_1q+f_2q^3+f_3q^5+\cdots$. From now on we always keep the first nonzero order of $f(q)$, provided that we want the simplest form of the effective continuum theory. The important magnetoelectric terms in an effective theory should be low energy in nature. So the above magnetoelectric term can be written as $i\lambda_c f_1 q P_c[M^*_{(1)b}M_{(1)c,a}-\text{c.c.}\pm(1)\to(2)]$, where λ_c is a function of the parameters—temperature, lattice constant, spin-orbit coupling constant, etc. Such an expression can be easily shown to be equivalent to

$$\lambda_c P_c[M_{(1)b}(y)\partial_y M_{(1)c,a}(y) - \partial_y M_{(1)_b}(y)M_{(1)c,a}(y)] \pm \lambda_c P_c[(1)\to(2)], \quad (33)$$

after a Fourier transform where λ_c is the intrachain magne-

toelectric coupling. Now let us consider the term $P_a[M^*_{(1)b}S_{(1)c,a}+\text{c.c.}\mp(1)\rightarrow(2)]$. There, prefactor i is absent so the lowest-order term we keep in $f(q)$ is f_0. After the Fourier transform, the real-space expression is

$$\lambda_a P_a[M_{(1)b}(y)M_{(1)c,a}(y)\mp(1)\rightarrow(2)], \tag{34}$$

where λ_a is the intrachain magnetoelectric coupling. Like λ_c, it is a constant depending on the known parameters mentioned earlier. Having considered Eqs. (27)–(30) as examples, we now focus on the interchain terms in real space using the same method. We then have for Eqs. (31) and (32)

$$\beta_a P_a[\vec{M}_{(1)}\times\partial_y\vec{M}_{(2)}+\vec{M}_{(2)}\times\partial_y\vec{M}_{(1)}]_b, \tag{35}$$

$$\beta_c P_c[\vec{M}_{(1)}\times\vec{M}_{(2)}]_b, \tag{36}$$

where β_a and β_c are the interchain couplings.

Physically, the magnetoelectric coupling must involve more than one atom in real space. The two terms expressed in Eq. (34) are therefore out of consideration. We observe that the term represented by Eq. (36) is independent of the spin structure along the chain but dependent only on the relative phase between the two chains, which is not reasonable. Therefore, the terms represented by Eqs. (33) and (35) are the only possible magnetoelectric coupling terms in the effective theory. These are the interactions which are considered in Sec. V.

Before we move on to Sec. V, let us comment on the relation and the deviation between the proposed theory and the existing phenomenological theory,[18] which adopts $\vec{P}\cdot[(\vec{M}\cdot\nabla)\vec{M}-(\vec{\nabla}\cdot\vec{M})\vec{M}]$ as the general form for the magnetoelectric coupling. It can be verified that the intrachain coupling term $i\lambda_c f_1 q P_c[M^*_{(1)b}M_{(1)c}-\text{c.c.}+(1)\rightarrow(2)]$ is, up to a factor, simply the first part of $\vec{P}\cdot[(\vec{M}\cdot\nabla)\vec{M}-(\vec{\nabla}\cdot\vec{M})\vec{M}]$ that has P_c in it. This explains why one can still understand the zero-field data using the previous theory. However, our theory deviates from the existing one[18] in all the other magnetoelectric terms. For example, the term $iP_a[M^*_{(1)b}M_{(1)a}-\text{c.c.}+(1)\rightarrow(2)$, which is a term in $\vec{P}\cdot[(\vec{M}\cdot\nabla)\vec{M}-(\vec{\nabla}\cdot\vec{M})\vec{M}]$ and used in explaining the development of P_a in a magnetic field, cannot be found in our set of magnetoelectric couplings. In fact, one can check that this term violates the symmetry invariance under the operation 2_c and cannot feature in any theory related to this compound. This tells us that, even if the spins do flop to the *ab* plane, one still *cannot* use the old theory to explain the ferroelectricity flop from the *c* to the *a* axis.

Why does the existing phenomenological theory[18] fail in $LiCu_2O_2$? One of the postulates of the theory is that the ferroelectricity is coupled to a single spin chain, or many independently contributing spin chains. One can do a symmetry analysis to recover the magnetoelectric term $\vec{P}\cdot[(\vec{M}\cdot\nabla)\vec{M}-(\vec{\nabla}\cdot\vec{M})\vec{M}]$. The lattice symmetry group here is the symmetry group of a single chain, obviously different from the one for a real multiferroic. However, the application of the theory is not limited to the systems consisting of only independent chains. Mathematically, one can show that, in a system that has at least one one-dimensional (1D) representation of the little group, this theory may be applied. In those systems one can always define $M_\alpha=\Sigma_{\text{unit cell}}S_{i\alpha}$ and it is automatically a symmetry adapted variable. Physically, in doing this one has considered the unit cell as one single spin, hence ignoring the details of the lattice, and making the complex lattice a simple lattice with only one spin per site. This simplified system can always be viewed as a set of single spin chains. Even if such a condition is met, Ref. 18 might still not be the *right* theory but only an *allowed* theory. Nevertheless, there are multiferroics where there are no 1D representations for the little group. In such cases, $M_\alpha=\Sigma_{\text{unit cell}}S_{i\alpha}$ is no longer a symmetry adapted variable and therefore the complex lattice cannot be simplified. Here the single chain theory always fails to meet the requirement of symmetry invariance and therefore must be excluded. One example of this is RMn_2O_5, which have one 2D representation. Another example is $LiCu_2O_2$ as demonstrated in this paper. It also may be true that systems with an antiferromagnetic alignment along a certain crystallographic direction do not have 1D representations while those without such modulation do have 1D representations and therefore may be explained using the conventional phenomenological theory. However, due to the diversity and complexity of all multiferroic materials, we do not have proof to back such a generalization.[26]

To end this discussion, we wish to clarify that there is a distinction between "interchain magnetoelectric coupling" and "interchain spin exchange." The latter is necessary for long-range magnetic order as in the three-dimensional (3D) Heisenberg model. The former can be totally absent in models for materials such as $TbMnO_3$ and $MnWO_4$,[5] where each spin-spiral chain can contribute independently to the ferroelectricity. In these cases a 1D chain that has a spiral magnetic structure is adequate enough to generate the ferroelectricity. The Katsura-Nagaosa-Balatsky model[27] for $RMnO_3$ and Lorenz's 1D anisotropic classical Heisenberg model for $MnWO_4$ are examples of this. For $LiCu_2O_2$ we propose an interchain magnetoelectric coupling which is an interaction term that involves more than one spin-spiral chain.

V. EFFECTIVE HAMILTONIAN

Based on the arguments of Sec. IV, we state the simple effective Hamiltonian which can explain the basic phenomena observed in the $LiCu_2O_2$ experiments.[8] In particular we provide an explanation for the polarization flip in the presence of an external magnetic field. The effective Hamiltonian that we propose includes only two terms. One term involves the intrachain coupling which is responsible for the electric polarization along the *c* axis. The other term involves the interchain coupling that is responsible for the electric polarization along the *a* axis. The magnetoelectric coupling Hamiltonian H_{ME} is given by

$$H_{\text{ME}}=\lambda_c P_c[\vec{M}_{(1)}\times\partial_y\vec{M}_{(1)}+\vec{M}_{(2)}\times\partial_y\vec{M}_{(2)}]_a + \beta_a P_a[\vec{M}_{(1)}\times\partial_y\vec{M}_{(2)}+\vec{M}_{(2)}\times\partial_y\vec{M}_{(1)}]_b, \tag{37}$$

where the symbols have the same meaning as before. Both

these terms satisfy the underlying lattice and magnetic symmetry requirements.

The proposed effective Hamiltonian [Eq. (37)] explains the basic physics of the $LiCu_2O_2$ system. First, in the absence of any external magnetic field according to the neutron-scattering experiments,[8,9] the spins lie on the bc plane. We have for the ground-state spin configuration, $\vec{M}_{(1)o}$ and $\vec{M}_{(2)o}$, in the two chains

$$\vec{M}_{(1)o} = S[0, \cos(qy), \sin(qy)], \tag{38}$$

$$\vec{M}_{(2)o} = S[0, \cos(qy + \delta\phi), \sin(qy + \delta\phi)], \tag{39}$$

where $\delta\phi$ is the phase difference between the spin configurations of the two chains. Based on Eq. (37) this spin configuration leads to an electric polarization along the c axis,

$$P_c \propto [\vec{M}_{(1)} \times \partial_y \vec{M}_{(1)} + \vec{M}_{(2)} \times \partial_y \vec{M}_{(2)}]_a = \text{const}. \tag{40}$$

Second, in the presence of an applied magnetic field along the b axis, the spin should flip to the ac plane when the field is larger than a certain critical value. This spin-flop transition is expected in a very general magnetic model with relatively isotropic couplings and spiral magnetism. This is similar to the spin-flop transition in the antiferromagnetic Heisenberg model in the presence of a Zeeman magnetic field. Therefore the expected ground-state spin configuration in the two chains is

$$\vec{M}_{(1)o} = S[\cos(qy), 0, \sin(qy)], \tag{41}$$

$$\vec{M}_{(2)o} = S[\cos(qy + \delta\phi), 0, \sin(qy + \delta\phi)]. \tag{42}$$

Based on Eq. (37), this spin arrangement leads to an electric polarization along the a axis (see Sec. VII for a discussion on twinning and its consequences for our model) when the spin structure in both the spin chains are in phase, that is, $\delta\phi = 0$,

$$P_a \propto [\vec{M}_{(1)} \times \partial_y \vec{M}_{(2)} + \vec{M}_{(2)} \times \partial_y \vec{M}_{(1)}]_b = \text{const}. \tag{43}$$

The theoretical model developed above suggests that the polarization in the two crystallographic direction comes from two different types of coupling. The polarization along the c axis arises from the intrachain coupling while the polarization along the a axis stems from the interchain coupling. Furthermore, in formulating this model we do not include strong anisotropy in the spin model to explain the flop transition of the electric polarization in the presence of an applied external magnetic field.

VI. SPIN STRUCTURES AND ELECTRIC POLARIZATION

Since there is no general consensus on the zero-field magnetic structure of the $LiCu_2O_2$ compound, we provide here a discussion for the various experimentally proposed magnetic structures.[8–11] We explore the consequences of the effective trilinear magnetoelectric coupling (see Sec. V) for each spin arrangement—the Masuda structure,[10] the Park and Seki structure,[8,9] and the Gippius structure.[11] We impose no constraints on the magnetoelectric couplings except that the two components of magnetization that enter the coupling should be different due to the fact that ferroelectricity is generated in the presence of *noncollinear* magnetic structure in this compound. Using the proposed model we then calculate the static ferroelectric polarization produced. The three magnetic structures, when written in the real space are Masuda, $\vec{M}_{(i)}(y) = M[\cos(qy + \phi_i), \sin(qy + \phi_i), 0]$; Park and Seki, $\vec{M}_{(i)}(y) = M[0, \cos(qy + \phi_i), \sin(qy + \phi_i)]$; and Gippius, $\vec{M}_{(i)}(y) = M[\sin(qy + \theta_0)\cos(qy + \phi_0), \cos(qy + \theta_0), \sin(qy + \theta_0)\sin(qy + \phi_0)]$, where we leave the relative phase between the two spin chains to be arbitrary. We Fourier transform the expressions and have for the Masuda structure, $M_{(i)a}(q) = 1/2 \exp(i\phi_i)$, $M_{(i)b}(q) = 1/(2i)\exp(i\phi_i)$; for the Park and Seki structure, $M_{(i)c}(q) = 1/2 \exp(i\phi_i)$, $M_{(i)b}(q) = 1/(2i)\exp(i\phi_i)$; and for the Gippius structure, $M_{(i)a}(2q) = \exp(i(\theta_0 + \phi_0))/(4i)$, $M_{(i)a}(0) = \sin(\theta - \phi)/2$, $M_{(i)b}(q) = \exp(i\theta_0)/2 M_{(i)c}(2q) = -\exp(i(\theta_0 + \phi_0))/4$, $M_{(i)c}(0) = \cos(\theta - \phi)/2$. Inserting these Fourier components into the expressions for magnetoelectric couplings [Eqs. (27)–(32)], we calculate the space-averaged ferroelectricity in all three directions. The results are reported in Table IV.

TABLE IV. Electric polarization predictions for the various experimentally proposed spin structures (Refs. 8–11) based on our proposed effective trilinear magnetoelectric coupling, Eq. (37). The electric polarization is represented by (P_a, P_b, P_c) along the (a, b, c) crystallographic direction.

Spin structures and corresponding polarization			
Polarization	Masuda	Park and Seki	Gippius
P_a	0	0	$\neq 0$
P_b	0	0	0
P_c	0	$\neq 0$	0

From the above results we conclude that the structure suggested by Park *et al.*[8] and Seki *et al.*[9] is most likely to be the real magnetic structure, as the polarization calculated using a general magnetoelectric coupling produces the correct direction (along the c axis). A similar calculation with the magnetic field applied along the b axis cannot reliably predict the direction in which the ferroelectricity exists. This is due to the effect of twinning and we discuss this issue in the next section.

VII. CONSEQUENCES OF TWINNING

The experimental data on $LiCu_2O_2$ (Ref. 8) reveal that the compound exhibits a unique behavior of generating an electric polarization parallel to the applied external magnetic-field direction. In reality, one of the difficulties for the experiments on this material is the twinning of the crystal (see Fig. 2), which renders the synthesis of a large single crystal extremely intractable.[28] Twinning is caused by the coincidental equality between the crystallographic a axis and the doubled b axis, $a \approx 2b$. With such twinning, it is difficult to

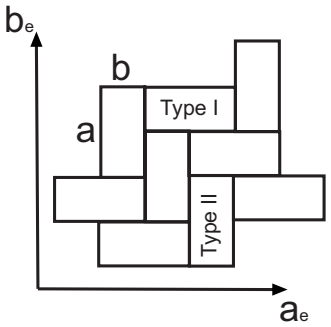

FIG. 2. A typical zoom-in picture of the twinned crystal structure is shown. The long direction of the patch has length a and the short direction has length b. We choose the horizontal axis as the experimental a axis, denoted by a_e, which is either along the real a axis (for type-I patches) or along the real b axis (for type-II patches). We define the direction perpendicular to a_e as the experimental b axis, b_e.

identify unambiguously the orientation of some important order parameters in the neutron-scattering experiments. For example, the ac-plane spiral cannot be distinguished from the bc-plane spiral. Furthermore, if there is a nonzero ferroelectric order in the ab plane, we cannot know whether it is along the a axis or along the b axis. To clarify the situation, in this section, we discuss the effect of twinning and its consequences on the predictions from our model.

To begin with, one has to realize that there are two possible orientations in a sample. We call these type-I and type-II patches. We choose the horizontal axis as the experimental a axis, denoted by a_e, which is either along the real a axis (for type-I patches) or along the real b axis (for type-II patches). We define the direction perpendicular to a_e as the experimental b axis, b_e. Notice that twinning happens only in the ab plane so the c axis can be determined unambiguously. We still define the experimental c axis, c_e, but keep in mind that it is the same as the crystallographic c axis. The static properties at zero magnetic field are not affected by the twinning as both kinds of patches contribute to the c_e axis polarization.

The situation becomes subtle if a magnetic field is applied along the b_e axis. We discuss its effect on both the type-I and type-II patches separately. For type-I patches, the crystallographic axes are aligned with the experimental axes; therefore the magnetic field is applied along b axis. According to the analysis above, there is a spin-flop transition at a certain field, which was experimentally determined as $H_c \sim 3$ T (see Fig. 3 of Ref. 8). At the transition, the polarization of these patches will also flop to a axis, which qualitatively explains the $\sim 50\%$ drop in P_c at $H \sim 4$ T, as half of the patches are type-I patches. For the type-II patches, a magnetic field along b_e is actually applied to its a axis. For a magnetic spiral on the bc plane, which was the ground state of the compound in zero field, a magnetic field along the a axis can only tilt the spiral toward its direction and change the spiral from a coplanar spiral to a conical spiral. There is no spin-flop transition in type-II patches, and the ferroelectric moment is always along the c axis. However, the magnitude of it could be tuned by the magnetic field to become smaller. A naive picture to see this is that, with the magnetic field becoming larger and larger, the spiral is more and more tilted so that the bc-plane components of the spins become smaller, thus making the ferroelectricity also decrease [using Eq. (35)]. This explains the experimental fact that with the field higher than 4 T, there is still a remnant c-axis polarization, which survives up to 9 T and is only as small as 1/4 of the zero-field polarization. Combining the consideration of both kinds of patches, we claim that the sudden drop of P_c at ~ 4 T and the nonzero remnant P_c are both effects of crystal twinning. For an idealistic single crystal, we predict that one sees a complete polarization flop from the c axis to the a axis. A good example of a complete flop is $TbMnO_3$ at very low temperature at $H \approx 5$ T.

VIII. ELECTROMAGNON SELECTION RULES

In this section, using the phenomenological Hamiltonian we predict a selection rule to be obeyed by the hybrid excitations of phonon and magnon termed as electromagnons.[29] It is hoped that these electromagnon excitations can be experimentally detected in future experiments.

The selection rule can be stated as follows: electromagnetic waves that are polarized perpendicular to the bulk electric polarization can be absorbed. To be more specific in zero magnetic field only those electromagnetic waves that are polarized along the crystallographic a axis can couple to the magnons. However, with an applied magnetic field along the b axis, only those waves polarized in the crystallographic c axis can couple to the magnons.

The selection rules can be obtained in the following manner. We first consider the case with the external magnetic field absent. The dynamics of the system can be derived by assuming a small deviation in the ground-state properties

$$\vec{P} = \vec{P}_o + \vec{u}, \tag{44}$$

$$\vec{M}_{(1)} = \vec{M}_{(1)o} + \delta\vec{M}_{(1)}, \tag{45}$$

$$\vec{M}_{(2)} = \vec{M}_{(2)o} + \delta\vec{M}_{(2)}, \tag{46}$$

where $\vec{P}_o$, $\vec{M}_{(1)o}$, and $\vec{M}_{(2)o}$ are the ground-state values, and the small deviations are indicated by $\vec{u}$, $\delta\vec{M}_{(1)}$, and $\delta\vec{M}_{(2)}$. Energy minimization requires that the first-order terms vanish in the ground state. We therefore study the second-order terms in the perturbation expansion to see how the dynamical degrees of freedom are coupled. Also the spin being a length-preserving vector, we know that $\delta\vec{M}_{(i)} \perp \vec{M}_{(i)o}$. Defining $\vec{n}_1 = [0, \cos(qy), \sin(qy)]$, $\vec{n}_2 = [0, -\sin(qy), \cos(qy)]$, we have $\delta\vec{M}_1 = m_1^{(1)}\vec{n}_2 + m_2^{(1)}\vec{a}$ (where $\vec{a}$ is the unit vector along the a axis). We now consider the second-order coupling that involves $\vec{u}_c$ and $\delta\vec{M}_{(1)}$ derived from Eq. (37),

$$\begin{aligned} u_c[\delta\vec{M}_{(1)} \times \partial_y\vec{M}_{(1)o} - \partial_y\delta\vec{M}_{(1)} \times \vec{M}_{(1)o}]_a \\ = S^2 u_c\{q[m_1^{(1)}\vec{n}_2 + m_2^{(1)}\vec{a}] \times \vec{n}_2 \\ - [\partial_y m_1^{(1)}\vec{n}_2 - q m_1^{(1)}\vec{n}_1 + \partial_y\vec{a}] \times \vec{n}_1\}_a \end{aligned}$$

$$= S^2 \partial_y m_1 u_c. \tag{47}$$

In momentum space the above expression can be written as

$$S^2 u_c(-\vec{k})(-ik_y) m_1^{(1)}(\vec{k}). \tag{48}$$

From this we infer that the zero mode phonon $u_c(\vec{k}=0)$ does not couple to the magnons. Therefore, if we compute the optical conductivity Im $G_{uu}(\vec{k}=0,\omega)$ in the lowest order (second order), the coupling does not contribute. This shows that when $P_c \neq 0$ the phonons along the same direction do not couple to the magnons. These phonons make no contribution to the electromagnons that may be observed in an optical conductivity measurement. However, the higher-order terms are still coupled. A similar type of result can be obtained with the terms involving $\delta\vec{M}_{(2)}$. This verifies the first part of our selection rule by showing that, when an electric polarization is present along the c axis, only the phonons polarized along the a axis can couple to the magnons to generate the electromagnons.

The coupling between the phonons polarized along the a axis and the magnons can be derived as follows. For u_a, from Eq. (37) we have

$$u_a[\delta\vec{M}_{(1)} \times \partial_y \vec{M}_{(2)o} - \vec{M}_{(2)o} \times \partial_y \delta\vec{M}_{(1)}]_b$$
$$= S^2 u_a[-q\cos(qy) m_2^{(1)} + \sin(qy)\partial_y m_2^{(1)}]. \tag{49}$$

Therefore the total effective Hamiltonian H_d^{eff} describing the dynamics of the phonon and the magnon can be written as

$$H_d^{\text{eff}} = \sum_p \left\{ h\omega_0 b^\dagger(p) b(p) + \frac{\rho p^2}{2} \sum_i m_2^{\dagger(i)}(p) m_2^{(i)}(p) + \frac{\lambda_a S^2}{2}[b^\dagger(p+q) + b^\dagger(p-q)][-q m_+(p) - p m_+(p)] \right\}, \tag{50}$$

where h is the Planck constant, $\rho \sim J$ (the effective magnetic coupling strength in the magnetic chain), q is the incommensurate wave vector, ω_0 is the bare phonon energy, b_p is phonon annihilation operator, and $m_+ = \Sigma_i m_2^{(i)}$.

A qualitative understanding of the electromagnon frequency for the $LiCu_2O_2$ compound can be obtained by performing a spin-wave analysis. The analysis is done for the case when the optical phonon frequency is much larger than the magnon frequency of interest. This implies that if we measure the ac conductivity versus frequency we will observe a peak at the frequency of the magnon. We should note that two points justify the neglect of the dynamic lattice degrees of freedom, the displacement field u, for the $LiCu_2O_2$ system. First, the optical phonon frequency is much higher than the magnon frequency. Second, the magnetoelectric coupling is very small compared to the other multiferroics, for example, in the 113 systems. This makes it unnecessary to explicitly include the dynamic degrees of freedom in the dielectric displacement.[27]

We now perform a standard spin-wave analysis[27] about the ground state to find the frequency at the desired wave vector, $\vec{k}=\vec{Q}$. The model Hamiltonian for $LiCu_2O_2$ proposed in Ref. 10 is

$$H = \sum_{i,j} (J_1 \vec{S}_{i,j} \cdot \vec{S}_{i+1,j} + J_2 \vec{S}_{i,j} \cdot \vec{S}_{i+2,j} + J_4 \vec{S}_{i,j} \cdot \vec{S}_{i+4,j} + J_\perp \vec{S}_{i,j} \cdot \vec{S}_{i,j+1}) + D S_\perp^2. \tag{51}$$

Here we have included an easy-plane anisotropy which generally exists due to the anisotropy of the lattice. Moreover this term favors the easy plane of spin alignment in the ground state, say, the bc plane in zero field, but the ac plane in a strong magnetic field along the b axis. To solve for the spin-wave dispersion we employ the rotating frame of reference coordinate system, writing the spin vector at any site relative to the other rotating one as

$$\vec{S}_{i,j} = S_{i,j}^\xi \vec{e}_x + [S_{i,j}^\eta \cos(\vec{Q}\cdot\vec{R}_{i,j}) + S_{i,j}^\zeta \sin(\vec{Q}\cdot\vec{R}_{i,j})]\vec{e}_y + [-S_{i,j}^\eta \sin(\vec{Q}\cdot\vec{R}_{i,j}) + S_{i,j}^\zeta \cos(\vec{Q}\cdot\vec{R}_{i,j})]\vec{e}_z. \tag{52}$$

In the above equation the magnetic propagation vector is given by $\vec{Q}=(\frac{\pi}{a}, \frac{2\pi\xi}{b}, 0)$, where $\xi=-0.174$ is the spiral modulation along the chain. Inserting the above form for the spin vector, we recast the Hamiltonian in terms of S^ξ, S^η, and S^ζ components. We then compute the effective magnetic-field components using the formula $\vec{H}_{\text{eff}} = -\vec{\nabla}_{\vec{S}_{i,j}} H$. We then solve for the equation of motion for the spin components using the effective magnetic-field equations and spin components in terms of the Holstein-Primakoff formalism listed below:

$$S_{m,n}^\xi = \sqrt{\frac{S}{2}}(a_{m,n} + a_{m,n}^*), \tag{53}$$

$$S_{m,n}^\eta = -i\sqrt{\frac{S}{2}}(a_{m,n} - a_{m,n}^*). \tag{54}$$

The equations of motion are given by

$$\hbar \dot{S}_{m,n}^\xi = S_{m,n}^\eta H_{\text{eff}}^\zeta - S_{m,n}^\zeta H_{\text{eff}}^\eta, \tag{55}$$

$$\hbar \dot{S}_{m,n}^\eta = S_{m,n}^\zeta H_{\text{eff}}^\xi - S_{m,n}^\xi H_{\text{eff}}^\zeta, \tag{56}$$

where in the above equation we set $S_{i,j}^\zeta = S$ since it is the direction in which the spin average points. Using the equations for the effective magnetic field, the spin components, and finally Fourier transforming, we obtain the dispersion as

$$-\frac{\hbar}{2S}\dot{S}^\xi(\vec{q}) = S^\eta(\vec{q})\left(J(\vec{Q}) - \frac{J(\vec{Q}+\vec{q}) + J(\vec{Q}-\vec{q})}{2}\right), \tag{57}$$

$$-\frac{\hbar}{2S}\dot{S}^\eta(\vec{q}) = S^\xi(\vec{q})[J(\vec{q}) - J(\vec{Q}) + D], \tag{58}$$

where we define $J(\vec{q}) = J_1\cos(q_b b) + J_2\cos(2q_b b) + J_4\cos(4q_b b) + J_\perp\cos(q_a a)$, where q_a and q_b refer to the a and b components of the wave vector. From the equations above it is obvious that at $\vec{q}=\vec{Q}$ we have

$$\hbar\omega(\vec{Q}) = 2S\sqrt{\left(\frac{J(2\vec{Q}) + J(0)}{2} - J(\vec{Q})\right)D}. \tag{59}$$

The above electromagnon dispersion indicates that the frequency is proportional to the square root of the easy-plane anisotropy D. In zero field, the easy plane is the bc plane. With an applied magnetic field along the a axis, this field will effectively increase the anisotropy in the form of $D \sim D_0 + H_a^2/2\rho$, where ρ is the spin stiffness. This should lead to a hardening of the electromagnon frequency (a right shift of the peak in the ac-conductivity measurement). If the magnetic field is applied along the b axis, it effectively diminishes the easy-plane anisotropy in the form of $D \sim D_0 - H_b^2/2\rho$. Therefore, one must observe the softening along with the increase in the magnetic field and at the point where the frequency becomes zero, the magnon mode becomes unstable, and the spin-flop transition happens

The above mechanism explains the observed phase transition at a certain magnetic field along the b axis as the destabilization of one electromagnon mode. In the high-field phase, the spins are lying in the ac plane, making the ac plane an easy plane described by an anisotropy term. In this phase, increasing the field along the b axis will increase the easy-plane anisotropy, whereas applying a field along the a axis will decrease the anisotropy. Therefore, we predict that the electromagnon hardens with an increase in magnetic field along the b axis, and softens with an increase in magnetic field along the a axis. This is opposite to what we should see in the low-field phase.

IX. SUMMARY AND CONCLUSIONS

In this paper we analyze the possible types of magnetoelectric coupling in the recently studied multiferroic compound $LiCu_2O_2$. Based on a group theoretical analysis we construct a multi-order-parameter phenomenological model for the double-chain zigzag structure. We show that an interchain magnetoelectric coupling belonging to the same unit cell explains the experimental results of Park *et al.*[8] This constructed model for the multiferroic $LiCu_2O_2$ compound can explain the polarization flip from the c to the a axis with the applied magnetic field along the b axis. The model can relate the flop of the spin-spiral plane with the direction of the electric polarization. We conclude that the zero-field structure observed by Seki *et al.*[9] is the correct one. We also provide a discussion on twinning and elucidate how it leads to difficulties in unambiguously predicting the direction of the ferroelectric polarization. The model makes specific selection rule predictions about the hybrid phonon and magnon excitations called electromagnons. We predict that the electromagnon peaks measured in an ac-conductivity measurement are field dependent and behave in opposite ways in the $P \| a$ and $P \| c$ phases. However, since the value of the polarization in this material is rather weak, it will require a very high-resolution spectroscopy measurement to observe the electromagnons in the actual system.

The model we propose in this paper could be oversimplified. However, at present only a limited set of experimental results are available for this compound. We believe this phenomenological model is a step toward understanding the magnetoelectric coupling effects observed in the $LiCu_2O_2$ compound. It is open to future experiments to determine the relevance of the other magnetoelectric coupling terms which we derived in this paper based on a group theoretical calculation.

ACKNOWLEDGMENTS

J.H. acknowledges the extremely useful discussions with S. W. Cheong.

*cfang@purdue.edu
†tdatta@aug.edu
‡hu4@physics.purdue.edu

[1] T. Kimura, T. Goto, H. Shintani, K. Ishizaka, T. Arima, and Y. Tokura, Nature (London) **426**, 55 (2003).
[2] N. Hur, S. Park, P. A. Sharma, J. S. Ahn, S. Guha, and S. W. Cheong, Nature (London) **429**, 392 (2004).
[3] T. Goto, T. Kimura, G. Lawes, A. P. Ramirez, and Y. Tokura, Phys. Rev. Lett. **92**, 257201 (2004).
[4] T. Lottermoser, T. Lonkai, U. Amann, D. Hohlwein, J. Ihringer, and M. Fiebig, Nature (London) **430**, 541 (2004).
[5] B. Lorenz, Y. Q. Wang, Y. Y. Sun, and C. W. Chu, Phys. Rev. B **70**, 212412 (2004).
[6] D. Higashiyama, S. Miyasaka, N. Kida, T. Arima, and Y. Tokura, Phys. Rev. B **70**, 174405 (2004).
[7] G. Lawes *et al.*, Phys. Rev. Lett. **95**, 087205 (2005).
[8] S. Park, Y. J. Choi, C. L. Zhang, and S.-W. Cheong, Phys. Rev. Lett. **98**, 057601 (2007).
[9] S. Seki, Y. Yamasaki, M. Soda, M. Matsuura, K. Hirota, and Y. Tokura, Phys. Rev. Lett. **100**, 127201 (2008).
[10] T. Masuda, A. Zheludev, A. Bush, M. Markina, and A. Vasiliev, Phys. Rev. Lett. **92**, 177201 (2004).
[11] A. A. Gippius, E. N. Morozova, A. S. Moskvin, A. V. Zalessky, A. A. Bush, M. Baenitz, H. Rosner, and S.-L. Drechsler, Phys. Rev. B **70**, 020406(R) (2004).
[12] A. B. Harris and G. Lawes, *The Handbook of Magnetism and Advanced Magnetic Materials*, edited by H. Kronmuller and S. Parkin (Wiley, New York) (to be published).
[13] M. Kenzelmann, A. B. Harris, S. Jonas, C. Broholm, J. Schefer, S. B. Kim, C. L. Zhang, S.-W. Cheong, O. P. Vajk, and J. W. Lynn, Phys. Rev. Lett. **95**, 087206 (2005).
[14] A. B. Harris, Phys. Rev. B **76**, 054447 (2007).
[15] M. Kenzelmann and A. B. Harris, Phys. Rev. Lett. **100**, 089701 (2008).
[16] A. S. Moskvin and S. L. Drechsler, EPL **81**, 57004 (2008).
[17] A. S. Moskvin, Y. D. Panov, and S. L. Drechsler, arXiv:0801.1975 (unpublished).
[18] M. Mostovoy, Phys. Rev. Lett. **96**, 067601 (2006).
[19] R. Berger, A. Meetsma, S. van Smaalen, and M. Sundberg, J. Less-Common Met. **175**, 119 (1991).
[20] S. Zvyagin, G. Cao, Y. Xin, S. McCall, T. Caldwell, W. Moulton, L.-C. Brunel, A. Angerhofer, and J. E. Crow, Phys. Rev. B **66**, 064424 (2002).
[21] B. Roessli, U. Staubb, A. Amatoc, D. Herlachc, P. Pattisond, K.

Sablinae, and G. A. Petrakovskiie, Physica B **296**, 306 (2001).
[22] T. Goto, T. Kimura, G. Lawes, A. P. Ramirez, and Y. Tokura, Phys. Rev. Lett. **92**, 257201 (2004).
[23] L. E. Svistov, A. I. Smirnov, L. A. Prozorova, O. A. Petrenko, A. Micheler, N. Buttgen, A. Ya. Shapiro, and L. N. Demianets, arXiv:cond-mat/0603617 (unpublished).
[24] T. Masuda, A. Zheludev, B. Roessli, A. Bush, M. Markina, and A. Vasiliev, Phys. Rev. B **72**, 014405 (2005).
[25] K.-Y. Choi, S. A. Zvyagin, G. Cao, and P. Lemmens, Phys. Rev. B **69**, 104421 (2004).
[26] C. Fang and J. Hu, EPL **82**, 57005 (2008).
[27] H. Katsura, N. Nagaosa, and A. V. Balatsky, Phys. Rev. Lett. **95**, 057205 (2005).
[28] S. W. Cheong (private communication).
[29] A. B. Sushkov, R. V. Aguilar, S. Park, S.-W. Cheong, and H. D. Drew, Phys. Rev. Lett. **98**, 027202 (2007).